Title
Cardiovascular Histopathology of a 11-Year Old with Mucopolysaccharidosis VII Demonstrates Fibrosis, Macrophage Infiltration, and Arterial Luminal Stenosis.

Authors
Lew, Valerie
Pena, Louis
Edwards, Robert
et al.

Publication Date
2018

DOI
10.1007/8904_2017_43

Peer reviewed

JIMD Reports
DOI 10.1007/8904_2017_43

RESEARCH REPORT

Cardiovascular Histopathology of a 11-Year Old with Mucopolysaccharidosis VII Demonstrates Fibrosis, Macrophage Infiltration, and Arterial Luminal Stenosis

Valerie Lew • Louis Pena • Robert Edwards • Raymond Y. Wang

Received: 05 April 2017 / Revised: 19 June 2017 / Accepted: 22 June 2017 / Published online: 13 July 2017

Abstract Mucopolysaccharidosis type VII (MPS VII) is caused by β-glucuronidase deficiency, resulting in lysosomal accumulation of glycosaminoglycans (GAGs) and multisystemic disease. We present cardiovascular gross and histopathology findings from a 11-year-old MPS VII male, who expired after developing ventricular fibrillation following anesthesia induction. Gross anatomic observations were made at autopsy; postmortem formalin-fixed paraffin-embedded samples of the carotid artery, aorta, myocardium, and valves were sectioned and stained with hematoxylin-eosin, Verhoeff-Van Gieson, CD68, and trichrome stains. Gross heart findings include an enlarged, dilated heart, mitral valve prolapse with thick, shortened chordae tendinae, and thickened aortic valve cusps. The aorta contained raised intimal plaques mimicking conventional atherosclerosis. Cardiac myocytes included hypertrophic nuclei, subendocardial fibrosis, and increased interfascicular collagen. Coronary lumens were 40–70% stenosed by fibrointimal hyperplasia containing storage material-laden cells, $CD68^+$ macrophages, and fragmented elastin laminae. Similar findings were visualized in aortic intimal plaques. We confirm that arterial plaques, elastin fragmentation, and activated $CD68^+$ macrophage infiltration occur in human MPS VII, consistent with previously observed findings in murine and canine MPS VII. We also confirm ultrasonographically observed carotid intimal-medial thickening is an in vivo correlate of histopathologic vascular fibrointimal hyperplasia. MPS VII patients should be regularly monitored for cardiac disease, with methods such as Holter monitors and stress testing; MPS VII-directed treatments should effectively address cardiovascular disease.

Communicated by: Frits Wijburg

V. Lew
UC Riverside School of Medicine, Riverside, CA 92521, USA

L. Pena
Los Angeles County Department of Medical Examiner-Coroner, Los Angeles, CA 90033, USA

L. Pena
Hidalgo Medical Services, Lordsburg, NM 88045, USA

R. Edwards
Department of Pathology & Lab Medicine, University of California, Irvine School of Medicine, Orange, CA 92868, USA

R.Y. Wang
Department of Pediatrics, University of California, Irvine School of Medicine, Orange, CA 92868, USA

R.Y. Wang (✉)
Division of Metabolic Disorders, Children's Hospital of Orange County, Orange, CA 92868, USA
e-mail: rawang@choc.org

Introduction

The mucopolysaccharidoses (MPSs) are inherited lysosomal storage diseases caused by deficiencies of enzymes involved in catabolism of glycosaminoglycans (GAGs). MPS type VII is caused by a deficiency of the lysosomal enzyme β-glucuronidase, which results in systemic accumulation of GAGs, specifically chondroitin sulfate (CS), dermatan sulfate (DS), and heparan sulfate (HS). Due to the ubiquitous nature of these GAGs, clinical manifestations of MPS VII include varying degrees of nonimmune hydrops fetalis, cognitive impairment, corneal clouding, airway obstruction, hepatosplenomegaly, orthopedic disease, and cardiovascular disease (Montaño et al. 2016). Even amongst MPSs, MPS VII is a rare condition, affecting 1 in every 345,000–2,000,000 live births (Muenzer 2011).

Sudden death has been described in two older patients, and corresponding reports of cardiovascular histopathology are also minimal (Vogler et al. 1994; Metcalf et al. 2010; Bigg et al. 2013; Gniadek et al. 2015). We describe the cardiovascular histopathology findings in a 11-year-old boy with MPS VII who died after sustaining ventricular tachycardia during a dental procedure under anesthesia, and relate the findings to findings in animal models of MPS VII that may shed light upon pathogenesis of MPS-associated cardiovascular disease. An up to date summary compiling hypothesis from literature on MPS VII pathogenesis is included to demonstrate the limited research.

Materials and Methods

Human Subjects

Consent for retrospective chart review and postmortem tissue donation was obtained from parents (Children's Hospital of Orange County IRB #100109, approved 12 Apr 2010).

Pathology

Tissue samples of the heart, ascending and descending aorta, rib cartilage, and spinal cord were frozen at −80°C. Additional formalin-fixed, paraffin embedded tissue samples from the Los Angeles County Coroners' office were sectioned and stained.

Histopathology

Tissue samples frozen in OCT were sectioned on a Leica CM3050 cryostat and stained with hematoxylin and eosin. Cytochemical stains for elastic fibers (Verhoeff-Van Gieson stain), glycosaminoglycan (Alcian Blue stain pH 2.5), collagen (Mallory Trichrome stain), and immunohistochemical stains for anti-human CD68 were performed on a Ventana Benchmark Ultra autostainer. Immunohistochemical staining was developed with peroxidase-based detection.

Results

Case Report

This patient was briefly reported in Montaño et al. (2016) as patient 12 (Montaño et al. 2016). His prenatal history was significant for hydrops fetalis noted at 8 months' gestation, and he was born at 38 weeks' gestational age due to pregnancy-induced hypertension and maternal proteinuria. Neonatal respiratory failure necessitated intubation and mechanical ventilation until the hydrops resolved. Organomegaly, thrombocytopenia, conjugated hyperbilirubinemia, and bilateral inguinal hernias were also present in the neonatal period leading to diagnosis of MPS VII.

He was lost to follow-up until 7 years of age, when he presented for medical attention for his MPS due to progressive behavioral difficulties and painful bilateral hip dysplasia. He had recurrent otitis media requiring ear tube implantation, hepatosplenomegaly, kyphoscoliosis, and obstructive sleep apnea. Urinary GAGs were quantitatively elevated at 32.9 mg/mmol creatinine (reference range <12 mg/mmol creatinine) and qualitatively demonstrated excess CS, DS, and HS. Molecular sequencing of the β-glucuronidase gene *GUSB* identified compound heterozygous, previously unreported c.295G>A/c.866G>A (p.V99M/W289X) variants.

The patient had quarterly electrocardiograms, echocardiograms, and cardiology evaluations. His initial echocardiogram at age 7.5 years showed mild aortic insufficiency, mild-moderate mitral insufficiency, mild left ventricular (LV) dilation, and normal fractional shortening (FS) of 35%. He was placed on enalapril due to the mitral insufficiency. Over the next 4 years, serial echocardiograms identified thickening of the mitral and aortic valves, mild mitral valve prolapse, mildly impaired LV relaxation, then mild-moderate diminished LV systolic function with an ejection fraction of 49% (reference range, >58%). At age 8.8 years, carotid ultrasonography identified greatly increased carotid intima media thickness (cIMT) of 0.50 mm on the right and 0.53 mm on the left compared to controls (mean control cIMT 0.48 mm, standard deviation 0.034 cm) (Wang et al. 2011).

His behavioral difficulties made it difficult to adequately keep up with his dental care, and the patient was therefore admitted for oral cleaning under anesthesia. He was administered Sevoflurane, and shortly after, he spontaneously developed ventricular tachycardia that rapidly degenerated to ventricular fibrillation. Efforts to resuscitate the patient were unsuccessful. Further pathology investigation identified primary cardiac etiology as cause of death.

Histopathology

Parental consent was given for postmortem studies. Weighing 275 g, more than twice the mean for age (122 g) (Hamill et al. 1979), the heart and especially the left ventricle were grossly enlarged and dilated. The mitral valve revealed ballooning of the leaflets with thick and shortened chordae tendinae. The aortic valve cusps were also thickened. Raised intimal plaques were visualized throughout the ascending and descending aorta. Noncardiac gross findings included cerebral edema, mucous plugging

of the conducting airways of the lung, and hepatosplenomegaly.

Microscopically, the sinoatrial, atrioventricular nodes, and conduction system were unremarkable. However, the myocardium contained hypertrophic cardiomyocytes with characteristic "boxcar" nuclei, prominent subendocardial fibrosis, and increased interfascicular collagen, consistent with chronic ischemic heart disease (Geer et al. 1980). Severe myxomatous degeneration (red arrowheads, Fig. 1a–c) and fibrosis (white arrowheads, Fig. 1b) were visualized in the mitral and aortic valves. The surface of the mitral valve was rich with numerous $CD68^+$ macrophages, which are usually not present in normal mitral valves (Fig. 1c: brown-stained cells marked with *m*).

Coronary lumens were 40–70% stenosed by intimal hyperplasia (Fig. 2a, b) that was shown to be composed of glycosaminoglycan-rich matrix (Fig. 2c: blue periodic acid-Schiff staining marked with *g*), storage-laden cells (Fig. 2d, examples marked with red arrowheads), fibrosis (Fig. 2d: blue Trichrome staining), fragmented elastin laminae (Fig. 2e: white arrowheads), and $CD68^+$ macrophages (Fig. 2g: brown-stained cells marked with *m*). None of the macrophages demonstrated lipid vacuole-laden cytoplasm and the hyperplastic regions showed no cholesterol-clefting. These findings are in dual contrast to normal arterial media, which has continuous sheets of elastin fibers and no macrophage infiltration, as well as to atherosclerotic plaques, which demonstrate "foamy" lipid-laden macrophages and cholesterol clefting (Miller 2014). Similar findings were seen focally in the aortic intimal plaques (Fig. 2e, f, h), though elastin fragmentation was less prominent compared to the coronary arteries.

Discussion

Cardiomyopathy and cardiac valve disease are very common manifestations of MPS VII, and frequently account for mortality in affected patients (Montaño et al. 2016). However, the pathogenesis of MPS VII cardiac disease is poorly understood due to scarce reports of human postmortem analyses. Of known histopathology reports of MPS VII patients (summarized in Table 1), most are in infants or fetal losses and very few focus upon the cardiovascular system. A MPS VII male who died suddenly at age 19 years demonstrated cardiac enlargement, thickening and calcification of the mitral and aortic valves, and plaques of the thoracic aorta and left anterior descending artery (Vogler et al. 1994). The aorta, which demonstrated cells distended with abundant storage material, was subsequently shown to have a large amount of elastin fragmentation (Metcalf et al. 2010). Cardiovascular pathology in a 28-year-old MPS VII patient who died in his sleep identified cardiac enlargement; myocardial interstitial fibrosis; pan-valvular thickening, fibrosis, and calcification; concentric narrowing of all coronary arteries with increased extracellular matrix, numerous $CD68^+$ macrophages, and mesenchymal cells distended by storage material (Gniadek et al. 2015). There was intimal-medial thickening of the aorta with disruption of the elastin laminae and scattered $CD68^+$ macrophages within.

Our patient demonstrated similar findings of cardiac enlargement and dilatation, subendocardial and interfascicular fibrosis, valve thickening, coronary artery stenosis and aortic plaques both demonstrating prominent intimal-medial hyperplasia, cellular GAG accumulation, $CD68^+$ macrophages, and fragmentation of the elastin laminae. Strikingly, these abnormalities were present at 11 years of age, indicating significant progression of MPS VII cardiovascular disease long before patients reach adulthood. The additional finding of carotid artery intimal-medial hyperplasia confirms the utility of carotid ultrasonography in identifying MPS-related cardiovascular disease in vivo. The pathologic findings (subendocardial myocardial fibrosis, dilated/hypertrophic cardiomyopathy, and anesthesia-induced hemodynamic changes) may all be manifestations

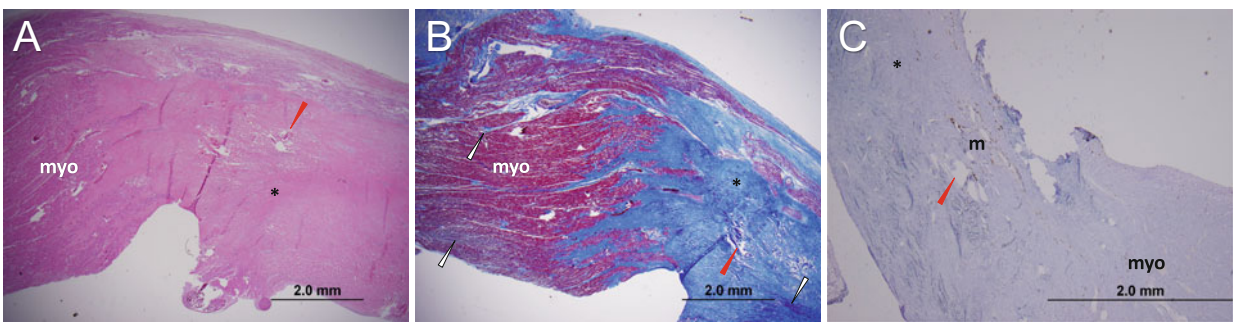

Fig. 1 Mitral valve and myocardial histopathology with (**a**) hematoxylin-eosin, (**b**) trichome stain, and (**c**) CD68 immunohistochemistry. Labels: *myo* myocardium, *asterisk* mitral valve, *m* macrophages. Myxomatous degeneration (*red arrowheads*), myocardial and valvular fibrosis (*white arrowheads*), and macrophage infiltration into valve parenchyma (*brown-stained cells*) are noted

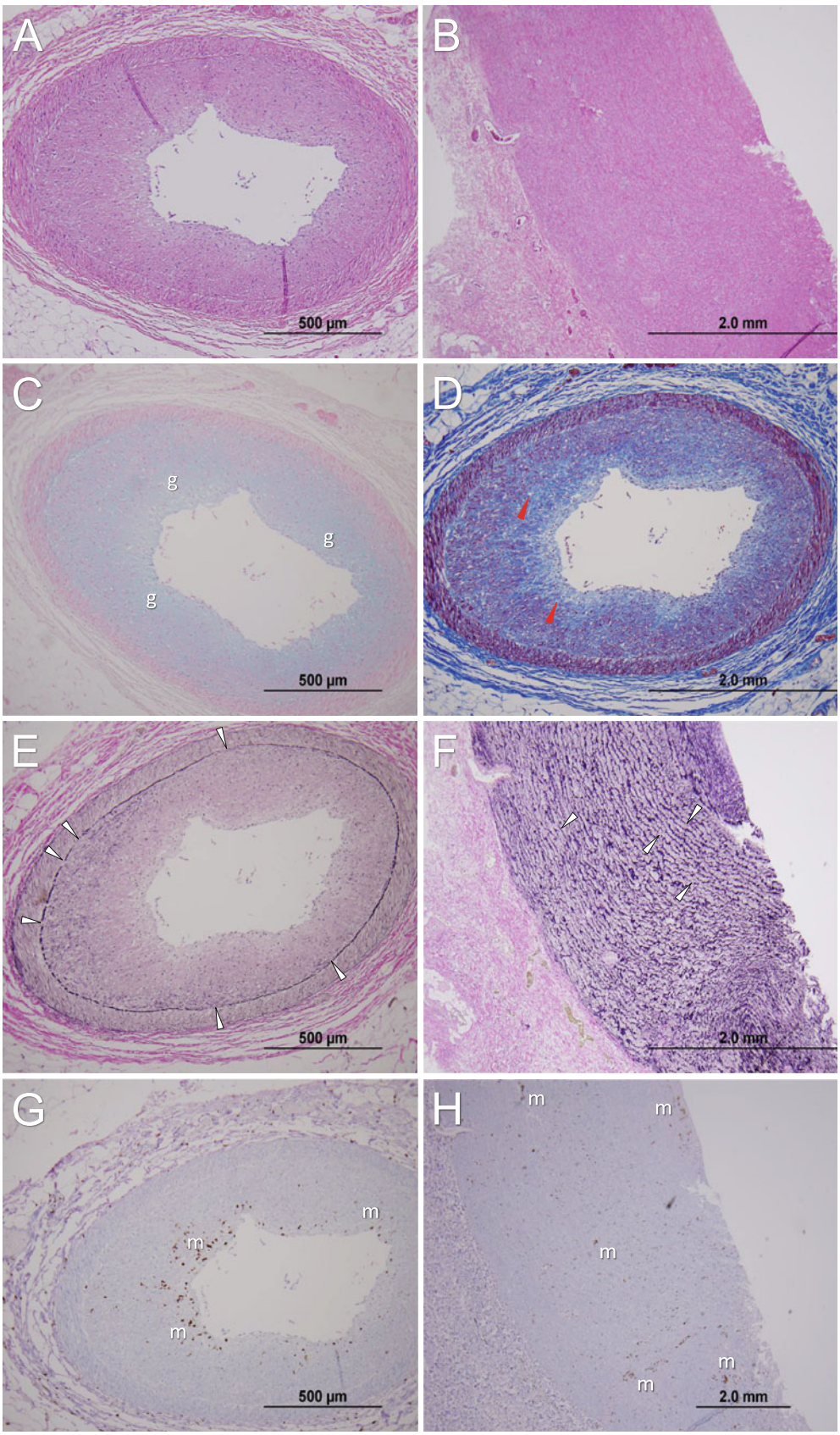

Fig. 2 Prominent luminal stenosis is visualized in hematoxylin-eosin stained (**a**) coronary artery and (**b**) ascending aorta. The stenosing

of longstanding, ongoing ischemic heart disease and have contributed to the patient's fatal dysrhythmia (Toda et al. 2001).

While MPS VII cardiovascular lysosomal storage begins prenatally, the progression and pathogenesis of cardiomyopathy, valvular dysfunction, vascular intimal-medial hyperplasia, and elastin fragmentation are being elucidated (Irani et al. 1983; Molyneux et al. 1997; Geipel et al. 2002; Venkat-Raman et al. 2006; Delbecque et al. 2009). The canine model of MPS VII, which has a severe, rapidly progressive phenotype, shows mitral and aortic valve thickening as early as 0.3 years (Sammarco et al. 2000), and demonstrates similar cardiovascular histopathology (Muenzer 2011). MPS VII canine aortas also demonstrate reduced elastin content, increased protease expression and enzymatic activity, coupled with the abundance of activated macrophages and increased expression of immune sensing receptors (toll-like receptor 4) and proinflammatory cytokines (TNFα). Findings implicating GAG-induced inflammation in MPS I canine cardiovascular disease are highly suggestive of a similar mechanism taking place in MPS VII (Khalid et al. 2016). The finding of $CD68^{+}$ macrophages, which promote inflammation, within valve tissue and infiltrating arterial parenchyma in this patient lend credence to this hypothesis. Additional functional or expression studies are needed to confirm this hypothesis, highlighting the importance of postmortem tissue collection to understand pathophysiology of MPS VII disease.

Acknowledgments The authors are grateful to the patient's parents for consenting to autopsy, and to Long Beach Memorial Hospital for obtaining autopsy consent. The authors are also grateful to the Los Angeles County Coroner's Office (Dan Anderson, Dr. Jason Tovar, Dr. Christopher Rogers, and Dr. Kevin Miller), and to Dr. Lisa Shane of Long Beach Miller Children's Hospital, for their efforts to make this publication possible. RYW is supported by the CHOC Children's Specialists Tithe Grant and the Brian and Caris Chan Family Foundation. The findings and conclusions in this chapter are those of the authors, and do not necessarily represent the official position of the County of Los Angeles or the Los Angeles County Department of the Medical Examiner-Coroner.

Synopsis

Significant cardiovascular disease (arterial fibrointimal stenosis, hypertrophic cardiomyopathy, valvular and myocardial fibrosis, and life-threatening dysrhythmias) was observed in a 11-year-old with mucopolysaccharidosis type VII; these findings indicate the importance of regular cardiology monitoring for MPS VII patients starting in early childhood.

Details of the Contributions of Individual Authors

- V.L. and R.Y.W. designed outline for manuscript as well as the figures
- L.P. performed postmortem
- L.P. and R.E. performed histopathology and interpretations
- V.L., L.P., R.E., and R.Y.W. wrote the manuscript

Name of the Corresponding Author

Raymond Y. Wang.

Competing Interest Statement

V.L., L.P., and R.E. have no conflicts of interest to declare. R.Y.W. is a study site principal investigator for a phase III study of recombinant human beta-glucuronidase for mucopolysaccharidosis type VII sponsored by Ultragenyx Pharmaceutical.

Details of Funding

This study was supported by CHOC Children's Specialists (V.L. and R.Y.W.), The Brian and Caris Chan Family Foundation (R.Y.W.), and The University of California-Riverside School of Medicine (V.L.).

Details of Ethics Approval

This report was conducted under the auspices of Children's Hospital of Orange County IRB #100109, approved 12 Apr 2010, renewed 17 Nov 2016.

A Patient Consent Statement

Consent for retrospective chart review and post mortem tissue donation was obtained from parents and is available for review upon request.

Fig. 2 (continued) lesions are composed of (**c**) glycosaminoglycans, as visualized by periodic acid-Schiff staining and denoted by *g*, (**d**) collagen fibrosis, and storage-containing "clear cells" (*red arrowheads*) as visualized by trichome staining. Elastin fragmentation (*white arrowheads*) was more notable in (**e**) the coronary artery than the (**f**) aorta. Macrophages, the CD68 (*brown*) staining cells marked with *m*, were also abundant within the lesions of (**g**) the coronary artery and (**h**) aorta but devoid of lipid-laden vacuoles

Table 1 Summary of the gross anatomy and histopathology findings of mucopolysaccharidosis type VII patients in the literature, including this report

MPS VII patient age of death (reference(s))	11 years (this report)	19 years (Vogler et al. 1994; Metcalf et al. 2010; Bigg et al. 2013)	28 years (Gniadek et al. 2015)	28 min (gest age unknown) (Irani et al. 1983)	Stillborn (32 weeks' gest) (Molyneux et al. 1997)	6 days (33 weeks' gest) (Geipel et al. 2002)	Fetal death (16 weeks' gest) (Venkat-Raman et al. 2006)	Termination (25 weeks' gest) (Delbecque et al. 2009)
Cardiac size	Enlarged	Slightly enlarged	Enlarged	n.m.	Dilatation	Hypertrophic	Normal	n.m.
Cardiac weight	275 g (nL 122 g)	400 g	484 g (nL 182–390 g)	n.m.	n.m.	n.m.	n.m.	n.m.
Mitral valve findings	Thick Fibrotic Myxomatous CD68+ cell infiltrate	Thick Calcified GAG storage Reduced collagen Neovascularized	Thick Fibrotic Nodular	n.m.	n.m.	n.m.	n.m.	n.m.
Aortic valve findings	Thick Fibrotic Myxomatous	Thick Nodular Calcified	Thick Nodular	n.m.	n.m.	n.m.	n.m.	n.m.
Coronary artery findings	Concentric narrowing Intimal thickening 40–70% stenosis CD68+ cell infiltrate	Eccentric narrowing 95% stenosis (left anterior descending)	Concentric narrowing Intimal thickening 75% stenosis (left anterior descending) 50–75% stenosis (circumflex) 75% stenosis (right coronary) CD68+ cell infiltrate	n.m.	n.m.	n.m.	n.m.	n.m.
Aortic findings	Visible plaque Intimal hyperplasia Elastin fragmentation CD68+ cells in plaque GAG accumulation	Visible plaques Elastin fragmentation Medial cells distended by storage Aortic dilatation	Visible thickening Intimal hyperplasia Elastin fragmentation CD68+ cells in plaque	n.m.	n.m.	n.m.	n.m.	Vacuolated aortic endothelium
Myocardium findings	Subendocardial fibrosis (prominent) Increased collagen, interfascicular Myocyte hypertrophy	n.m.	Thick myocardium Myocardial fibroelastosis Patchy interstitial fibrosis	n.m.	Vacuolated foamy myocardial cells	Vacuolated lysosomal overloading of myocytes	Normal microscopic exam of heart	n.m.
Other notes	Death from ventricular tachycardia Unremarkable SA/AV nodes	Death in sleep (aspiration vs. arrhythmia)	Death in sleep	Fetal hydrops GAG storage in cardiac capillary endothelium	Fetal hydrops	Fetal hydrops	Fetal hydrops	Fetal hydrops Vacuolated cardiac endothelium

Documentation of Approval from the Institutional Committee for Care and Use of Laboratory Animals (or Comparable Committee)

Not applicable (no animal studies).

References

Bigg PW, Baldo G, Sleeper MM, O'Donnell PA, Bai H, Rokkam VR, Liu Y, Wu S, Giugliani R, Casal ML, Haskins ME, Ponder KP (2013) Pathogenesis of mitral valve disease in mucopolysaccharidosis VII dogs. Mol Genet Metab 110:319–328

Delbecque K, Gaillez S, Schaaps JP (2009) Histopathological diagnosis of a type vii mucopolysaccharidosis after pregnancy termination. Fetal Pediatr Pathol 28(1):1–8

Geer JC, Crago CA, Little WC, Gardner LL, Bishop SP (1980) Subendocardial ischemic myocardial lesions associated with severe coronary atherosclerosis. Am J Pathol 98(3):663–680

Geipel A, Berg C, Germer U, Krapp M, Kohl M, Gembruch U (2002) Mucopolysaccharidosis VII (Sly disease) as a cause of increased nuchal translucency and non-immune fetal hydrops: study of a family and technical approach to prenatal diagnosis in early and late pregnancy. Prenat Diagn 22(6):493–495

Gniadek TJ, Singer N, Barker NJ, Spevak PJ, Crain BJ, Valle D, Halushka MK (2015) Cardiovascular pathologies in mucopolysaccharidosis type VII (Sly syndrome). Cardiovasc Pathol 24 (5):322–326

Hamill PV, Drizd TA, Johnson CL, Reed RB, Roche AF, Moore WM (1979) Physical growth: National Center for Health Statistics Percentiles. Am J Clin Nutr 32(3):607–629

Irani D, Kim HS, El-Hibri H, Dutton RV, Beaudet A, Armstrong D (1983) Postmortem observations on beta-glucuronidase deficiency presenting as hydrops fetalis. Ann Neurol 14(4):486–490

Khalid O, Vera MU, Gordts PL, Ellinwood NM, Schwartz PH, Dickson PI, Esko JD, Wang RY (2016) Immune-mediated inflammation may contribute to the pathogenesis of cardiovascular disease in mucopolysaccharidosis type I. PLoS One 11(3): e0150850

Metcalf JA, Linders B, Wu S, Bigg P, O'Donnell P, Sleeper MM, Whyte MP, Haskins M, Ponder KP (2010) Upregulation of elastase activity in aorta in mucopolysaccharidosis I and VII dogs may be due to increased cytokine expression. Mol Genet Metab 99(4):396–407

Miller DV (2014) Other pediatric cardiac conditions. In: Collins KA, Byard RW (eds) Forensic pathology of infancy and childhood. Springer, New York, pp 943–972

Molyneux AJ, Blair E, Coleman N, Daish P (1997) Mucopolysaccharidosis type VII associated with hydrops fetalis: histopathological and ultrastructural features with genetic implications. J Clin Pathol 50(3):252–254

Montaño AM, Lock-Hock N, Steiner RD, Graham BH, Szlago M, Greenstein R, Pineda M, Gonzalez-Meneses A, Coker M, Bartholomew D, Sands MS, Wang R, Giugliani R, Macaya A, Ketko AK, Ezgu F, Tanaka A, Arash L, Beck M, Falk RE, Bhattacharya K, Franco J, White KK, Mitchel GA, Cimbalistiene L, Holtz M, Sly WS (2016) Clinical course of sly syndrome (mucopolysaccharidosis type VII). J Med Genet 53(6):403–418

Muenzer J (2011) Overview of the mucopolysaccharidoses. Rheumatology 50(Suppl 5):v4–v12

Sammarco C, Weil M, Just C, Weimelt S, Hasson C, O'Malley T, Evans SM, Wang P, Casal ML, Wolfe J, Haskins M (2000) Effects of bone marrow transplantation on the cardiovascular abnormalities in canine mucopolysaccharidosis VII. Bone Marrow Transplant 25(12):1289–1297

Toda Y, Takeuchi M, Morita K, Iwasaki T, Oe K, Yokoyama M, Hirakawa M (2001) Complete heart block during anesthetic management in a patient with mucopolysaccharidosis type VII. Anesthesiology 95:1035–1037

Venkat-Raman N, Sebire NJ, Murphy KW (2006) Recurrent fetal hydrops due to mucopolysaccharidoses type VII. Fetal Diagn Ther 21(3):250–254

Vogler C, Levy B, Kyle JW, Sly WS, Williamson J, Whyte MP (1994) Mucopolysaccharidosis VII: postmortem biochemical and pathological findings in a young adult with beta-glucuronidase deficiency. Mod Pathol 7(1):132–137

Wang RY, Covault KK, Halcrow EM, Gardner AJ, Cao X, Newcomb RL, Dauben RD, Chang AC (2011) Carotid intima-media thickness is increased in patients with mucopolysaccharidoses. Mol Genet Metab 104(4):592–596